The Columbia Non-neutral Torus: A new experiment to confine nonneutral and positron-electron plasmas in a stellarator.

T. Sunn Pedersen, A. H. Boozer, J. P. Kremer, *Columbia University*
W. Reiersen, F. Dahlgren, N. Pomphrey, *Princeton Plasma Physics Laboratory*
W. Dorland, *University of Maryland*.

Introduction

Confinement systems that use magnetic field lines alone have several advantages over those that use magnetic and electric fields, such as the Penning trap, including the ability to confine positive and negative particles simultaneously, and the ability to confine light, energetic particles. Closed toroidal field line systems have been used to confine pure electron plasmas [1-4], and more recently, magnetic surface configurations have become of interest as confinement devices for non-neutral plasmas [5,6]. The physics of pure electron plasmas confined on magnetic surfaces is fundamentally different from previously studied configurations [6].

In contrast to other magnetic surface configurations, a stellarator has the advantage that it can be steady state, and does not require internal currents. This means that it can be operated at arbitrarily low density, which is an important advantage for making non-neutral and electron-positron plasmas, since these will be very low density compared to quasi-neutral fusion plasmas. A stellarator, the Columbia Non-neutral Torus (CNT), is currently being constructed specifically to investigate the physics of non-neutral plasmas confined on magnetic surfaces. This paper reviews the theory of non-neutral plasmas confined on magnetic surfaces, and discusses some of the experimental parameters that are of importance to a non-neutral stellarator experiment. We also present the design of the CNT stellarator, which is unique in that it will be ultrahigh vacuum, very low aspect ratio, and will require only four simple, circular planar coils.

Confinement of pure electron plasmas

The equilibrium of a pure electron plasma in a magnetic surface configuration is described by a self-consistent equation for the electrostatic potential [6]:

Eq. 1 $$\nabla^2\phi = \frac{e}{\varepsilon_0} N(\psi) \exp\left(\frac{e\phi}{T_e(\psi)}\right)$$

Here ψ is the magnetic surface coordinate, that is, each magnetic surface is described by ψ=*constant*. The temperature is taken to be constant on a magnetic surface due to rapid thermalization along field lines, $T_e=T_e(\psi)$. The function $N(\psi)$ indirectly specifies the density profile. The equilibrium plasma flow is:

Eq. 2 $$\vec{v}_e = \left(\frac{\vec{\nabla} p}{e n_e} - \vec{\nabla}\phi\right) \times \vec{B} \Big/ B^2 + \frac{v_{e\|}}{B}\vec{B}$$

It can be shown that this flow cannot cross the magnetic surfaces [6]. The parallel flow adjusts itself to make the total particle flux divergence free, even if the perpendicular particle flux is not. With closed toroidal field lines, or in a Penning trap, the parallel flow cannot do this, and hence, contours of constant density and electrostatic potential must coincide in order to keep the perpendicular particle flux divergence free.

The equilibrium electrostatic potential given by Equation 1 minimizes an energy-like quantity [7]:

Eq. 3 $U = \int \left(\frac{1}{2} \varepsilon_0 (\nabla \phi)^2 + N(\psi) T(\psi) \exp(e\phi / T(\psi)) \right) dV = \int \left(\frac{1}{2} \varepsilon_0 E^2 + p \right) dV$

The equilibrium electron density increases near positive image charges. Although this is what would be naively expected, it is in contrast to what happens in the Penning trap [8] and the pure toroidal field trap [9}, which have electrostatic potentials that maximize the potential energy, and the electron plasma tends to move away from positive image charges. However, the energy-like quantity that is minimized in equilibrium in a magnetic surface configuration is not the free energy, so this does not guarantee stability of all possible configurations. Further work is needed to develop proper stability criteria of pure electron plasmas confined on magnetic surfaces.

Confinement

Confinement in a non-neutral stellarator is limited by neoclassical diffusion, and possibly direct orbit losses, if the non-neutral stellarator does not possess quasi-symmetry. In addition to the curvature and ∇B drifts, the ExB drift also causes particles to drift away from the magnetic surfaces, to the extent that the electrostatic potential is not constant on a magnetic surface. The electrostatic potential contours do match very closely to the magnetic surfaces in any region with appreciable plasma density, unless the Debye length is large.

In addition to the rotational transform, the ExB drift will cause particles to move poloidally on magnetic surfaces, squeezing in their drift orbits. In the limit where this effect is dominant, a simple scaling estimate yields the following particle confinement time.

Eq. 4 $\tau_p > \tau_e \frac{a^4}{\lambda_D^4}$

Here τ_e is the electron collision time, and the estimate above is valid for small Debye lengths, and direct orbit losses (bad orbits) are neglected since the large electric field should prevent significant orbit losses.

During the initial formation phase of a pure electron stellarator plasma, the electric field will be weak, and the scaling law above will not hold. The magnetic surface configuration itself will provide excellent confinement of passing particles, but there will be some direct orbit losses until the space charge electric field becomes sufficient to significantly alter the particle orbits.

Confinement of partly neutralized and electron-positron plasmas.

A stellarator confines both positive and negative particles simultaneously whether space charge and internal currents are present or not. This allows the study of plasmas of arbitrary neutralization, a field of plasma physics that is currently largely unexplored. Positive particles, ions or positrons, will be very well confined in an electron-rich plasma, by the overall negative space charge as well as by the magnetic surfaces. As one slowly neutralizes the plasma, the electric field weakens, as the density rises. The electron confinement time will then be

Eq. 5 $\tau_p \approx \tau_e \frac{a^4}{\lambda_C^4}$

This is a similar scaling to that of a pure electron plasma, however, the Debye length λ_D is replaced by the Coulomb length,

Eq. 6 $\lambda_C^4 \equiv \frac{(n_e + n_p)^2}{(n_e - n_p)^2} \lambda_D^4$

Here, n_e is the electron density and n_p is the density of the positive species, assumed to be a proton or a positron. In a quasi-neutral plasma a/λ_C is on the order of 1 or less, whereas in a pure electron plasma, $a/\lambda_C=a/\lambda_D>>1$.
A partly neutralized plasma may be characterized by $a/\lambda_D>a/\lambda_C >> 1$. The confinement time given by Equation 5 is long in this limit, and that may allow significant accumulation of positrons injected into a stellarator containing an initially pure electron plasma, even with the relatively weak positron sources available today [10]. Hence, this may be an attractive way to create the first laboratory electron-positron plasma.
As predicted by this scaling, confinement can become very poor as the plasma becomes quasi-neutral, unless the stellarator has quasi-symmetry.

Important parameters for a non-neutral stellarator experiment
In order to guide the design of CNT, we have identified important physics parameters for a non-neutral stellarator. Specifically, we have focused on parameters of importance to confining pure electron plasmas. The most fundamental physics parameter of any plasma physics experiment is a/λ_D, where a is the smallest characteristic size of the plasma, in the case of a stellarator, the minor radius. In order for the electron cloud to be a plasma, $a/\lambda_D>>1$ should be satisfied. In a non-neutral plasma experiment, including CNT, this is a non-trivial constraint that requires careful matching of the injected electron energy to the plasma potential, or some method of cooling the plasma after it has been injected. $a/\lambda_D >> 1$ is particularly important in a non-neutral stellarator, given the predicted strong scaling of the confinement time with a/λ_D, Equation 4. Another important parameter is the time scale for ion accumulation due to ionization of background neutrals, τ_I. When $\tau_I>> \tau_p$, electron plasmas will decay before being significantly contaminated. When $\tau_I<< \tau_e$, ions will significantly neutralize an initially pure electron plasma before it decays away. It is desirable to maximize both time scales, since either one can trivially be decreased. A large τ_I will be achieved through the ultrahigh vacuum design and operation at low plasma
temperature. A large τ_p can be achieved by making the Debye length short compared to the system size, although there is a tradeoff involved which will be addressed in the following.

A key issue for a non-neutral plasma on magnetic surfaces is whether the plasma truly equilibrates on a magnetic surface through parallel dynamics faster than the ExB drift can take the plasma away from the magnetic surfaces. In a quasi-neutral plasma, this is basically always true, but the ExB drift can be very large in non-neutral plasmas. The time scale for perpendicular distortions is the ExB rotation time $\tau_\perp=2\pi a/(E/B)$. Any breaking of the parallel force balance will lead to plasma oscillations that are subsequently Landau damped in a finite temperature plasma. We approximate the parallel relaxation time $\tau_\parallel$ by the time it takes a thermal particle to move along the magnetic field to fully explore the magnetic surface. The ratio of the two time scales can then be expressed as:

Eq. 7 $$\frac{\tau_{ExB}}{\tau_\parallel}=\frac{\pi a/v_{ExB}}{\pi R/\iota v_{th}}\approx 2\sqrt{2}\varepsilon\iota\frac{\lambda_D}{a}\sqrt{\frac{n_B}{n}}=\varepsilon\iota B(2\sqrt{2}\frac{\lambda_D}{a}\sqrt{\frac{\varepsilon_0}{2mn}})$$

Here, $n_B=\varepsilon_0 B^2/2m_e$ is the Brillouin density. Since $\iota<1$, $a/R<1$, the conditions that $a/\lambda_D>>1$ and $\tau_\perp/\tau_\parallel >>1$ can only be satisfied simultaneously if $\sqrt{(n_B/n)}>>1$, which is well satisfied in most non-neutral plasma experiments. CNT is designed to operate in this regime as well.

Design of the Columbia Non-neutral Torus

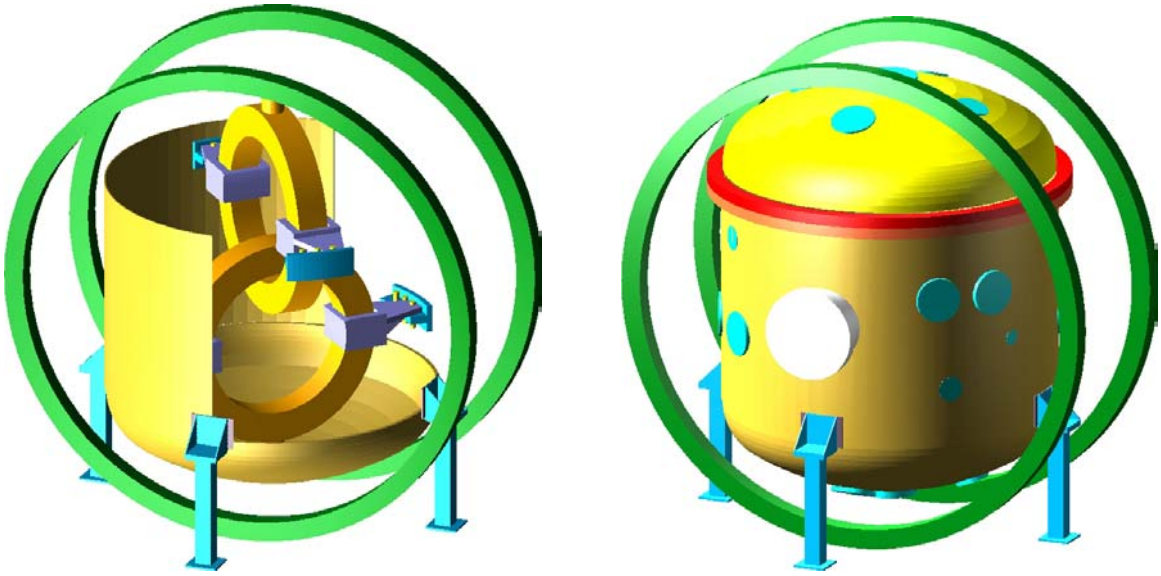

Figure 1. CAD drawings of the CNT experiment. The left figure is a cutaway view of the experiment, showing the PF coils (green), and the IL coils (yellow) inside the vacuum chamber, suspended from brackets (cyan) welded to the inner diameter of the vacuum chamber.

Design criteria

CNT is the first experiment specifically designed to study the physics of non-neutral and electron-positron plasmas confined in a stellarator. Based on the physics analysis just presented, and the mission of CNT as a University-based, inexpensive basic plasma physics experiment, CNT was designed according to the following criteria, roughly in order of importance:

- Good magnetic surface quality without large islands and ergodic regions, and resilience against magnetic field errors.
- Ultrahigh vacuum level, $<3*10^{-10}$ Torr, to prevent ion contamination and to make neutral interactions (such as neutral drag) negligible
- A value of $\varepsilon\iota B$ large enough to allow the ratio of perpendicular to parallel dynamical time scales to be large.
- A simple coil system that could be constructed quickly and inexpensively.
- Maximum physics flexibility, including the ability to change iota and shear profiles
- A simple and inexpensive vacuum chamber, but with good port access for vacuum pumps, diagnostics etc.
- The ability to access configurations with some magnetic shear

In contrast to fusion stellarator designs, we did not consider MHD stability, nor the degree of quasi-symmetry. MHD stability is likely irrelevant to the extremely tenuous plasmas studied in non-neutral plasma physics. Although quasi-symmetry would likely improve the confinement of non-neutral plasmas, it was decided that incorporation of quasi-symmetry would be make the coil design and fabrication too difficult to achieve with the relatively modest resources available for CNT. Also, the ExB drift will significantly alter the particle orbits, and if the number of Coulomb lengths can be made large enough, this should drastically reduce prompt orbit losses, even for a classical stellarator.

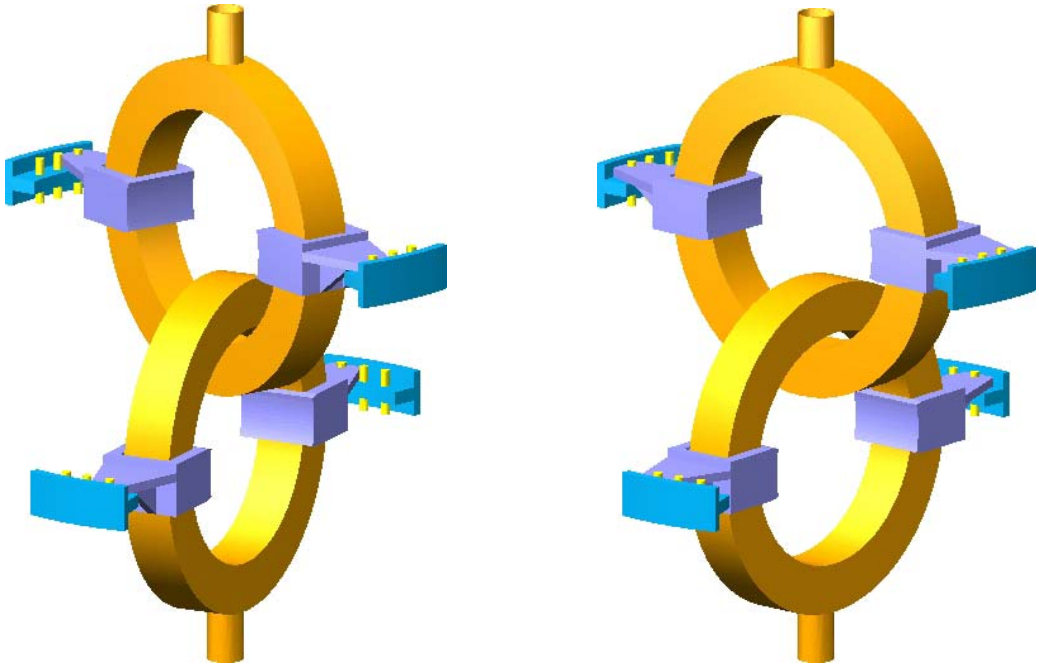

Figure 2. The interlocking coils mounted on their brackets. The left figure shows the two coils at an angle of 64^o, the right figure shows them at an angle of 88^o.

Coil design

The coil configuration is perhaps the simplest of any stellarator constructed, consisting only of four circular, planar coils, in two identical pairs, two interlocking (IL) coils, and two poloidal field (PF) coils, creating a two-period, low aspect ratio, classical stellarator configuration. The PF coils will be placed outside the vacuum chamber, will have an average radius of 108 cm, and will carry 30 to 60 kA-turns when the IL coils are at full current. They will be wound from rectangular copper conductor with a central water cooling channel. The two IL coils will be wound from rectangular hollow copper conductor, with an average coil radius of 40.5 cm, encased in a 316L stainless steel vacuum jacket. The two coils (see Figure 2) are placed vertically inside the vacuum chamber, each coil suspended on brackets welded to the vessel inner diameter, with the leads coming out through the top and bottom vacuum vessel flanges respectively. The vertical distance between the centers of the two IL coils will be 63 cm, and the angle between the two coils (the tilt angle) can be changed from 64^o to 88^o with an intermediate angle at 78^o. The design current is 170 kA-turns limited by a 200 kW DC power supply that will be used for the experiment. The added complexity of having the coils inside the vacuum chamber, especially with the strict requirements on the vacuum, was determined to be acceptable given the tremendous physics flexibility that comes from the ability to change the tilt angle. Equally important, it allowed an 8-fold increase in $\varepsilon\iota B$, by allowing more copper in the coils (increasing B for the same power supply), a larger IL coil tilt angle (which increases iota), and larger plasma minor radius (since the toroidal vacuum chamber was actually cutting off good magnetic surfaces. The cylindrical vacuum chamber, described in the following, was also more easily designed and manufactured than a toroidally shaped chamber would have been.

Magnetic field

Given the tenuous plasmas to be studied in CNT, only the vacuum magnetic fields were considered in the optimization of the magnetic fields for CNT. The basic configuration, consisting of two interlocking circular coils with two large PF coils, was developed by A.

Georgievsky, W. Reiersen et al., who based their configurations on a paper by Gourdon (1969). For the CNT design, a Fortran code was developed that takes advantage of the simple analytic formulas for the magnetic field of a current ring in terms of elliptic functions, eliminating the need to integrate the Biot-Savart formula along the current paths in the coils. This code was used to further optimize the design, to determine the optimum tilt angles and the optimum ratio of IL to PF coil currents, and to determine the susceptibility of the coil configurations to field errors caused by coil misalignments, winding transitions and current leads, and magnetic materials. Due to the analytic formulas, the code runs very fast, and these studies were performed on a standard Pentium-based workstation.

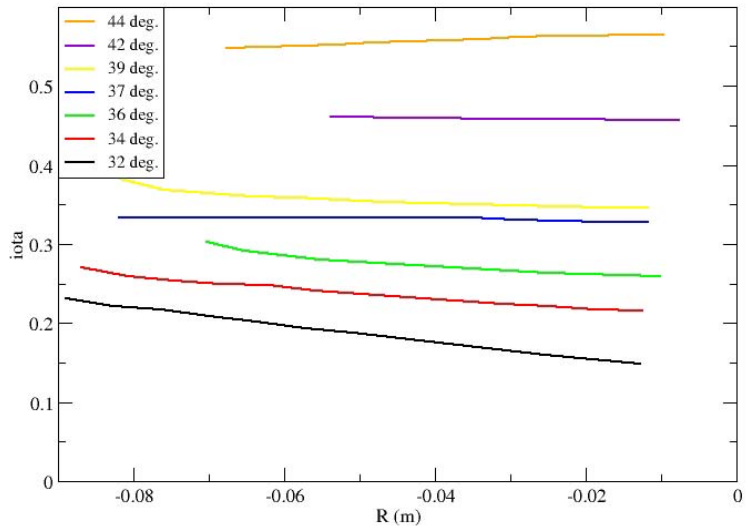

Fig. 3 Iota profiles for different angles between the IL coils. The major radius given is relative to the magnetic axis, and the angles given are half-angles between the IL coils (hence, 32^o on the figure means an angle of 64^o between the IL coils)

Iota profiles as a function of radius are shown for different tilt angles in Figure 3. It is clear that both iota and the magnetic shear vary significantly as functions of the tilt angle. For example, at an angle of 64^o (labeled as 32^o) on the figure, the central iota is approximately 0.15, with iota increasing to 0.23 at the plasma edge, whereas iota is nearly 0.6 on axis and slightly lower at the plasma edge at an IL coil angle of 88^o. At intermediate angles, iota is at an intermediate value and the configuration is nearly shear free. The field error analysis shows, not surprisingly, that configurations with iota going through low order rational values are much more sensitive to field errors [11]. These tend to have smaller volumes too, as outer surfaces break up due to these resonances. Based on this analysis, three working tilt angles were chosen: 64^o, 78^o, and 88^o. These tilt angles yield large magnetic surface volumes, relative resilience against field errors, and they scan the range of iotas from 0.15 to 0.57, and represent three generic shear configurations, reversed, near zero, and normal shear. Shear is predicted to be important in suppressing diocotron instabilities [12]. The three tilt angles also represent three rather different shapes, as shown in Figure 4.

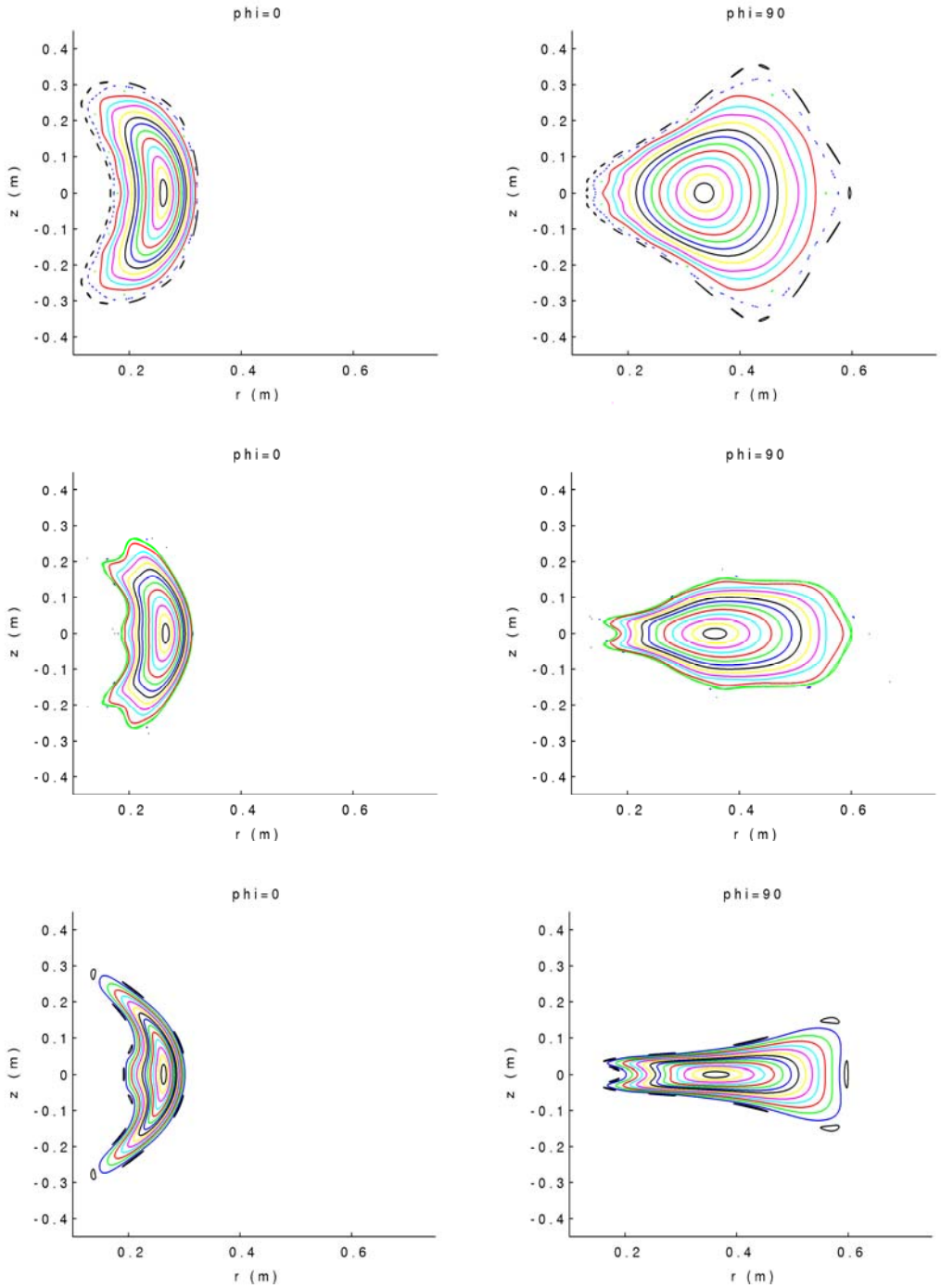

Figure 4. Poincare plots of the magnetic surfaces at the two principal toroidal planes (left and right) for the three chosen tilt angles, 64^{o}(top), 78^{o} (middle), and 88^{o} (bottom).

Vacuum chamber

Figure 5. The CNT vacuum chamber complete after leak tests at Ability Engineering in South Holland, IL, USA

The vacuum chamber, shown in Figure 5, is constructed from 316L stainless steel. It consists of an upright cylinder and two domed ends, with various ports. The top dome is removable for installation and repositioning of the IL coils. The inside of the vacuum chamber is electropolished, and only metal seals are used. It is bakeable to >200^{o}C and should reach a vacuum of $<2*10^{-10}$ Torr. The vessel has been leak checked and is awaiting final pumpdown to its base pressure after installation of the IL coil suspension brackets.

Expected plasma parameters.

A desirable operational point for initial pure electron plasma studies could be $n_e=10^{12}$ m^{-3} and $T_e=1$ eV. At this point, $a/\lambda_D=13.4$, $\tau_\perp/\tau_\parallel=18.5$, $\tau_I=2.7x\ 10^5$ s. The calculations here assume for simplicity that the neutrals are hydrogen atoms, which is not an unreasonable assumption as hydrogen often dominates in the ultrahigh vacuum range. The electron confinement time is more than one hour as predicted by Equation 4, dominated by electron-electron collisional transport. The ion contamination time is a very strong function of temperature though. At $T_e=5$ eV, $\tau_I=2.4$ s, still rather long, but now significantly shorter than the electron confinement time as well as the experimentally achievable pulse length.

Conclusion

CNT is being constructed specifically to study non-neutral and electron-positron plasmas confined in a stellarator. The design is a compromise between the need to build the device as easily and economically as possible, and the desire to access the most interesting parameter

regimes of such a device. We arrived at a design with a simple coil configuration, two adjustable in-vessel coils, a significant magnetic field strength, and an ultrahigh vacuum. The experiment is currently under construction.

Acknowledgements
The authors would like to acknowledge the contributions of F. Dahlgren, W. Reiersen and N. Pomphrey on the stellarator design, and W. Dorland on gyrokinetic simulations of electron-positron plasmas. This work was supported by the United States Department of Energy Grant DE-FG02-02ER54690.

References
1. Daugherty, J., Eninger, J., and Janes, G., *Phys. Fluids*, **12**, 2677 (1969).
2. Clark, W., Korn, P., Mondelli, A., and Rostoker, N., *Phys. Rev. Letters*, **37**, 592 (1976).
3. Zaveri, P., John, P., Avinash, K., and Kaw, P., *Phys. Rev. Letters*, **68**, 3295 (1992).
4. Stoneking, M. R., Fontana, P., and Sampson, R., *Phys. Plasmas*, **9**, 766 (2002).
5. Yoshida, Z., Ogawa, Y., Morikawa, J., et al., *AIP Conf. Proceedings*, **498**, 397 (1999).
6. Pedersen, T. S., and Boozer, A. H., *Phys. Rev. Letters*, **88**, 205002 (2002).
7. Pedersen, T. S., *Phys. Plasmas*, **10**, 334 (2003).
8. Notte, J., Peurrung, A. J., Fajans, J., Chu, R., and Wurtele, J. S., *Phys. Rev. Letters*, **69**, 3056 (1992).
9. O'Neil, T., and Smith, R., *Phys. Plasmas*, **1**, 2430 (1994).
10. Pedersen, T. S., Boozer, A. H., Dorland, W., Kremer, J. P., and Schmitt, R., *J. Phys. B*, **36**, 1029 (2003).
11. Kremer, J. P., Pedersen, T. S., Pomphrey, N., Reiersen, W., and Dahlgren, F., *Non-neutral Plasma Workshop, AIP Proceedings* (2003).
12. Kondoh, S., Tatsuno, T., and Yoshida Z., *Phys. Plasmas*, **8**, 2635, (2001)